HHS Public Access

Author manuscript

Nature. Author manuscript; available in PMC 2010 October 08.

Published in final edited form as:

Nature. 2010 April 8; 464(7290): 932–936. doi:10.1038/nature08944.

The kinetics of two dimensional TCR and pMHC interactions determine T cell responsiveness

Jun Huang[1,3], **Veronika I. Zarnitsyna**[1], **Baoyu Liu**[1], **Lindsay J. Edwards**[2], **Ning Jiang**[1,4], **Brian D. Evavold**[2], and **Cheng Zhu**[1]

[1]Coulter Department of Biomedical Engineering, Georgia Institute of Technology, Atlanta, GA 30332, USA

[2]Department of Microbiology and Immunology, Emory University School of Medicine, Atlanta, GA, 30322, USA

Abstract

The T cell receptor (TCR) interacts with peptide-major histocompatibility complexes (pMHC) to discriminate pathogens from self-antigens and trigger adaptive immune responses. Direct physical contact is required between the T cell and the antigen-presenting cell (APC) for cross-junctional binding where the TCR and pMHC are anchored on two-dimensional (2D) membranes of the apposing cells[1]. Despite their 2D nature, TCR-pMHC binding kinetics have only been analyzed three-dimensionally (3D) with a varying degree of correlation with the T cell responsiveness[2-4]. Here we use two mechanical assays[5,6] to show high 2D affinities between a TCR and its antigenic pMHCs driven by rapid on-rates. Compared to their 3D counterparts, 2D affinities and on-rates of the TCR for a panel of pMHC ligands possess far broader dynamic ranges that match that of their corresponding T cell responses. The best 3D predictor of response is the off-rate, with agonist pMHC dissociating the slowest[2-4]. In contrast, 2D off-rates are up to 8,300-fold faster, with the agonist pMHC dissociating the fastest. Our 2D data suggest rapid antigen sampling by T cells and serial engagement of a few agonist pMHCs by TCRs in a large self pMHC background. Thus, the cellular environment amplifies the TCR-pMHC binding to generate broad affinities and rapid kinetics that determine T-cell responsiveness.

The sustained interest in the kinetic analysis of TCR-pMHC interactions stems from a fundamental hypothesis that the interaction parameters play a central role in determining the

---

Correspondence and requests for materials should be addressed to C. Z. (cheng.zhu@bme.gatech.edu) or B. E. (bevavol@emory.edu).

[3]Present address: Department of Microbiology & Immunology and The Howard Hughes Medical Institute, Stanford University School of Medicine, Stanford, CA 94305, USA

[4]Present address: Department of Bioengineering, Stanford University, Stanford, CA, 94305, USA

Author contributions

N.J. and C.Z. initiated the kinetic study with F5 T cells; J.H. and C.Z. designed the kinetic study; J.H. and B.L. performed the micropipette experiments; V.I.Z. performed the BFP experiments and Monte Carlo simulations; L.J.E. and B.D.E. provided the T cells and conducted the functional study; J.H., V.I.Z., B.L. and C.Z. analyzed the data; B.D.E. and C.Z. wrote the paper with all authors contributing.

Author Information

Reprints and permissions information is available at www.nature.com/reprints. The authors declare no competing financial interests.

subsequent T cell response. We analyzed 2D TCR-pMHC interactions on naïve CD8+ OT1 T cells with the adhesion frequency[5,7] and thermal fluctuation[6,8] assays using a micropipette (Fig. 1a) and a biomembrane force probe (BFP, Fig. 1b). Both employ a red blood cell (RBC) as an adhesion sensor but the BFP also attaches a bead to the RBC. RBC or bead was functionalized with pMHC mutated to abrogate CD8 binding[9] (Fig. 1c) (Methods).

In the adhesion frequency assay[5,7], a T cell (Fig. 1a and b, right) was micro-manipulated to touch the RBC or bead with a controlled contact area and time. TCR-pMHC binding (if present) was observed visually by the RBC elongation (Movie M1) or detected by the bead displacement (Movie M2) on T cell retraction. To determine the likelihood of adhesion, the cell pair was moved repeatedly in and out of contact for a given contact time (t_c) to yield an adhesion frequency (P_a), i.e. the number of adhesions divided by the number of total contacts. The adhesion frequencies were specific because binding was abolished unless OT1 TCR and antigenic pMHC were used (Fig. 1d). Using a divalent straptavidin[10] (Di-SA) to ensure monomeric pMHC presentation (Fig. 1c) produced similar adhesion frequency as using a tetravalent wildtype streptavidin (WT-SA) to couple pMHC on RBCs (Fig. 1e), ruling out multimeric pMHC as the cause for high affinity binding (see below).

The 2D kinetic information is extracted by fitting an adhesion frequency curve measured using multiple cell pairs over a range of contact times with a mathematical model[5] (Fig. 2a-c), which derives separately two parameters ($m_r m_l A_c K_a$ and k_{off}) with good accuracy (Methods, Fig. S1). The 2D affinity K_a has a unit of area rather than volume, the unit of 3D affinity. We report the effective 2D affinity ($A_c K_a$, in μm^4) as it is evaluated together with the contact area A_c (a few percent of 3 μm^2 for micropipette or of 1 μm^2 for BFP). Adhesion frequency depends on the receptor (m_r) and ligand (m_l) densities. For example, three different OVA pMHC densities yielded three distinct adhesion levels (Fig. 2a) but the same affinity is derived (Fig. S2). The weaker ligands R4 (Fig. 2b) and G4 (Fig. 2c) required higher densities than OVA (Fig. 2a and c) yet still generated lower adhesion levels, indicating far lower affinities. The 2D off-rate k_{off} is not affected by the contact area or protein densities and is inversely proportional to the time $t_{1/2}$ required to reach half-maximal P_a level[5] (Method). The OVA curves in Fig. 2a reached equilibrium very rapidly, indicating a fast off-rate that required the BFP to measure accurately (Fig. 2c). The R4 (Fig. 2b) and G4 (Fig. 2c) curves rose more slowly, indicating slower off-rates. The effective 2D on-rate $A_c k_{on}$ ($= A_c K_a \times k_{off}$) equals the initial slope of the adhesion curve divided by the receptor and ligand densities. The much steeper initial slopes yet lower pMHC densities of the adhesion curves for OVA (Fig. 2a and c) than R4 (Fig. 2b) and G4 (Fig. 2c) indicate a much faster association of TCR with OVA.

In the thermal fluctuation assay[6,8] (Methods), association/dissociation events of TCR-pMHC bonds were identified by reduction/resumption of thermal fluctuations of the BFP bead because bond formation anchored the bead to the T cell, restricting its movements (Fig. S3 and Movie M3). The time from association to dissociation is bond lifetime t_b whose distributions line up in semi-log plots that linearize exponential decays, suggesting first-order dissociation of single-bonds for both OVA and G4 (Fig. 2d). Their respective off-rates equal the negative slope of the lines (Fig. 2d), which agree with the corresponding values from the adhesion curves (Fig. 2c). These results confirm that both assays measure stress-

free kinetics despite the use of force to break any bond present at the end of each contact cycle[5-8].

We compared 2D parameters of the OT1 TCR binding to a panel of pMHCs with increasing potencies[3] to the published 3D results[11,12] (Fig. 3). Regardless of receptor and ligand densities, the same monomeric binding model[5] fits adhesion curves at both 25 and 37 °C equally well for all ligands (Fig. S2) with higher temperature yielding higher affinities (Table 1). The effective 2D affinities from antagonist to agonist pMHC spanned three logs from 10^{-6}–10^{-3} μm^4, whereas that of null (VSV) pMHC was below 10^{-8} μm^4, the assay's detection limit[7] (Fig. 3a). In sharp contrast, the 3D affinities differ by only one log for the same ligand set (Fig. 3d), making it difficult to resolve ligand potencies from TCR kinetics. Further, the micromolar 3D K_D conveys an impression that TCR-pMHC binding is of low affinity; however, the OT1 (and F5, Fig. S4) TCR on naïve (and activated, Fig. S5) T cells have effective 2D affinities for agonist pMHCs similar to that of high affinity lymphocyte function-associated antigen (LFA)-1 for intercellular adhesion molecule (ICAM)-1[13], an interaction that provides strong adhesion for many immune functions.

The high 2D affinities of TCR for agonist pMHCs were driven by rapid 2D on-rates, which were even faster than that of P-selectin associating with P-selectin glycoprotein ligand (PSGL)-1[14], an interaction that requires a rapid on-rate to capture flowing leukocytes to inflamed vascular surfaces. Unlike the P-selectin-PSGL-1 interaction, however, the fast 2D on-rates for TCR-pMHC do not translate to fast 3D on-rates. In fact, the 3D TCR-pMHC on-rates[11,12] are >200-fold slower than the P-selectin-PSGL-1 3D on-rate[15]. The 3D TCR-pMHC on-rates are insensitive to the different peptides (Fig. 3e), suggesting that TCR binding is initiated by MHC contact[16]. By comparison, the 2D on-rates spanned four logs for the same ligand set (Fig. 3b), indicating the critical contribution of peptide contact to TCR-pMHC association. Thus, an important attribute of our measurements is their high sensitivity to discriminate binding kinetics for a range of closely related ligands.

The 2D off-rates (Fig. 3c) were 30-8300 fold faster than the corresponding 3D off-rates (Fig. 3f), with the value for TCR dissociating from OVA:H-2K^b (7.2 and 10.8 s^{-1} at 25 and 37 °C, respectively) comparable to that for L-selectin dissociating from PSGL-1 (10.2 s^{-1} at 25 °C), the most rapid selectin-ligand off-rate in both 2D and 3D, which is required for mediating fast rolling of leukocytes on vascular surfaces[6,17]. Again, the fast 2D off-rates for TCR-pMHC did not translate to fast 3D off-rates. In fact, OVA:H-2K^b dissociates from the OT1 TCR in a single step at 25 °C with a 3D off-rate of 0.022 s^{-1} but in two steps (i.e. requiring dimer formation) at 37 °C with a 3D off-rate of 0.0012 s^{-1} for the second step[11,12]. Most telling, the off-rates of stronger ligands are progressively faster in 2D but slower in 3D, displaying opposite trends (compare Fig. 3c and f). Thus, the TCR-pMHC off-rates and their relationships to ligand potency differ substantially between 2D and 3D.

To further test the hypothesis that TCR-pMHC kinetics determines T cell responsiveness, we measured the peptide concentration required to stimulate half-maximal T cell proliferation (EC_{50})[18] and plotted it vs. the 2D TCR binding parameters measured at 25 °C (Fig. 4a-c) and 37 °C (Fig. 4d-f). A strong correlation was found between $1/EC_{50}$ and all metrics of 2D kinetics, especially the affinities and on-rates, for their broad dynamic ranges

better match the wide range of functional responses. This is the first demonstration of the relevance of 2D TCR-pMHC binding kinetics to the functional response of T cells[19]. Besides T cell proliferation, a late-stage response assessed after three days of APC stimulation, the more proximal TCR downregulation response used in the previous 3D studies[3] also correlated well with our 2D parameters (Fig. S6).

The substantial differences between 2D and 3D kinetics for TCR-pMHC interactions are not seen in ligand binding of selectins and integrins. In light of the recent reports of TCR clustering on the cell surface in a cholesterol- and/or actin cytoskeleton-dependent fashion[20-23], we speculate that the T cell imposes unique regulations on the TCR organization, orientation, and/or conformation, which may affect the availability of TCR to binding or enable cooperative binding. While the 3D assays of purified molecules may measure their intrinsic kinetics independent of these regulatory mechanisms, our 2D assays may capture the impact of the cellular environment on TCR-pMHC interactions, which mimics the physiological situation (Fig. S7). Consistent with this view, we observed reduced effective 2D affinities of the OT1 TCR for OVA and G4 pMHCs by treatment with methyl-beta-cyclodextrin, a water-soluble cyclic heptasaccharide that can extract cholesterol from the plasma membrane[24] and alter TCR preclustered structures[22] (Fig. S8). Similar effects were observed by treatment with cholesterol oxidase, another cholesterol depletion agent (Fig. S9). Furthermore, the 2D affinities were also reduced by Latrunculin A, an inhibitor of actin polymerization (Fig. S10). Moreover, Monte Carlo simulations showed an increase in apparent affinity by cooperative binding if it is assumed that interaction of a pMHC with one TCR in a cluster increases the binding propensity of all members of the TCR cluster (Fig. S11). This form of cooperation is suggested by the observed memory effects of TCR-pMHC interaction such that adhesion in a past contact increases the likelihood of adhesion in the next contact[9].

The insufficient resolution of T cell responsiveness by 3D TCR-pMHC kinetics (e.g. Fig. 3d-f) has generated numerous models to explain the various functional outcomes[2-4,12,19,25-28]. The kinetic proofreading model proposed a serial scheme to amplify the small differences in the 3D TCR-pMHC off-rates[26]. Our data suggest that such amplification results in 2D on-rate, off-rate, and affinity that all match the T cell response to a given pMHC. The broad affinities and rapid kinetics of the 2D interactions meet the requirement for the T cell to scan with high speed and sensitivity the numerous self pMHCs on an APC to find, engage, and respond to antigen expressed at low numbers[29]. The observations of antigen sampling by a T cell from several APC[30] and the rapid microcluster formation between TCR and agonist pMHC further enforce how quickly the pMHC is interrogated to accumulate threshold signaling levels[20,23]. Microclusters of TCR coupled to its rapid 2D kinetics also allow a single pMHC to serially engage many TCRs in a short time. Note that here the term is used differently from the original model where serial engagement led to TCR internalization[27]. Although the lifetimes of individual TCR-pMHC bonds are brief because they dissociates rapidly, bonds also reform rapidly and frequently. Serial engagement allows both the quality and quantity of pMHC to be measured by the frequency of bond formation as it is proportional to the 2D affinity and the pMHC density. High bond formation frequency also accumulates a large fraction of engagement time. TCR clustering and cooperative binding could amplify serial engagement as it provides a high

local concentration of TCRs, thereby generating maximal recognition signal to trigger downstream events for T cell activation. Thus, our 2D TCR-pMHC kinetic data may provide a basis for a comprehensive model to explain self/non-self recognition, ligand discrimination, thymocyte selection, signal accumulation, feedback mechanisms, and TCR antagonism.

Method Summary

We used adhesion frequency assay[5] and thermal fluctuation assay[6] to measure the 2D kinetics of TCR-pMHC interaction on the cell membrane. The adhesion frequency assay employed a micropipette and a BFP, and the thermal fluctuation assay employed a BFP. T cells expressing monoclonal OTI or F5 TCR were purified from transgenic mice. Human RBCs directly (or indirectly through a glass bead) coated with pMHC via biotin-streptavidin coupling served as both a surrogate APC and a force sensor for detecting the TCR-pMHC interaction. The site densities of TCR and pMHC were measured by flow cytometry[7]. Monte Carlo simulations and pharmacological treatments were performed to study the effects of T cell membrane environment.

Supplementary Material

Refer to Web version on PubMed Central for supplementary material.

Acknowledgments

We thank the NIH Tetramer Core Facility at Emory University for providing MHC monomers, J. Altman for providing the H-2K^b mutant construct, G. Bao for providing the divalent streptavdin, as well as M. Davis and H.-T. He for commenting the manuscript. This work was supported by NIH grants AI38282 and AI060799 (to C.Z.) and AI056017 and National Multiple Sclerosis Society Grant RG4047-A-3 (to B.D.E.).

References

1. Dustin ML, Bromley SK, Davis MM, Zhu C. Identification of self through two-dimensional chemistry and synapses. Annu Rev Cell Dev Biol. 2001; 17:133–157. [PubMed: 11687486]
2. Davis MM, et al. Ligand recognition by alpha beta T cell receptors. Annu Rev Immunol. 1998; 16:523–544. [PubMed: 9597140]
3. Gascoigne NR, Zal T, Alam SM. T-cell receptor binding kinetics in T-cell development and activation. Expert Rev Mol Med 2001. 2001:1–17.
4. Stone JD, Chervin AS, Kranz DM. T-cell receptor binding affinities and kinetics: impact on T-cell activity and specificity. Immunology. 2009; 126(2):165–176. [PubMed: 19125887]
5. Chesla SE, Selvaraj P, Zhu C. Measuring two-dimensional receptor-ligand binding kinetics by micropipette. Biophys J. 1998; 75(3):1553–1572. [PubMed: 9726957]
6. Chen W, Evans EA, McEver RP, Zhu C. Monitoring receptor-ligand interactions between surfaces by thermal fluctuations. Biophys J. 2008; 94:694–701. [PubMed: 17890399]
7. Huang J, Edwards LJ, Evavold BD, Zhu C. Kinetics of MHC-CD8 interaction at the T cell membrane. J Immunol. 2007; 179(11):7653–7662. [PubMed: 18025211]
8. Chen W, Zarnitsyna VI, Sarangapani KK, Huang J. Measuring receptor-ligand binding kinetics on cell surfaces: from adhesion frequency to thermal fluctuation methods. Cell Mol Bioeng. 2009; 1:276–288. [PubMed: 19890486]
9. Zarnitsyna VI, et al. Memory in receptor-ligand-mediated cell adhesion. Proc Natl Acad Sci U S A. 2007; 104(46):18037–18042. [PubMed: 17991779]

10. Howarth M, et al. A monovalent streptavidin with a single femtomolar biotin binding site. Nat Methods. 2006; 3(4):267–273. [PubMed: 16554831]
11. Alam SM, et al. Qualitative and quantitative differences in T cell receptor binding of agonist and antagonist ligands. Immunity. 1999; 10(2):227–237. [PubMed: 10072075]
12. Rosette C, et al. The impact of duration versus extent of TCR occupancy on T cell activation: a revision of the kinetic proofreading model. Immunity. 2001; 15(1):59–70. [PubMed: 11485738]
13. Zhang F, et al. Two-dimensional kinetics regulation of αLβ2-ICAM-1 interaction by conformational changes of the αL-inserted domain. J Biol Chem. 2005; 280(51):42207–42218. [PubMed: 16234238]
14. Huang J, et al. Quantifying the effects of molecular orientation and length on two-dimensional receptor-ligand binding kinetics. J Biol Chem. 2004; 279(43):44915–44923. [PubMed: 15299021]
15. Mehta P, Cummings RD, McEver RP. Affinity and kinetic analysis of P-selectin binding to P-selectin glycoprotein ligand-1. J Biol Chem. 1998; 273(49):32506–32513. [PubMed: 9829984]
16. Wu LC, Tuot DS, Lyons DS, Garcia KC, Davis MM. Two-step binding mechanism for T-cell receptor recognition of peptide MHC. Nature. 2002; 418(6897):552–556. [PubMed: 12152083]
17. Nicholson MW, Barclay AN, Singer MS, Rosen SD, van der Merwe PA. Affinity and kinetic analysis of L-selectin (CD62L) binding to glycosylation-dependent cell-adhesion molecule-1. J Biol Chem. 1998; 273(2):763–770. [PubMed: 9422729]
18. Wang X, et al. Dynamics of proximal signaling events after TCR/CD8-mediated induction of proliferation or apoptosis in mature CD8+ T cells. J Immunol. 2008; 180(10):6703–6712. [PubMed: 18453590]
19. Zehn D, Lee SY, Bevan MJ. Complete but curtailed T-cell response to very low-affinity antigen. Nature. 2009; 458(7235):211–214. [PubMed: 19182777]
20. Campi G, Varma R, Dustin ML. Actin and agonist MHC-peptide complexdependent T cell receptor microclusters as scaffolds for signaling. J Exp Med. 2005; 202(8):1031–1036. [PubMed: 16216891]
21. Lillemeier BF, et al. TCR and Lat are expressed on separate protein islands on T cell membranes and concatenate during activation. Nat Immunol. 2009; 11(1):90–96. [PubMed: 20010844]
22. Schamel WW, et al. Coexistence of multivalent and monovalent TCRs explains high sensitivity and wide range of response. J Exp Med. 2005; 202(4):493–503. [PubMed: 16087711]
23. Yokosuka T, et al. Newly generated T cell receptor microclusters initiate and sustain T cell activation by recruitment of Zap70 and SLP-76. Nat Immunol. 2005; 6(12):1253–1262. [PubMed: 16273097]
24. Zidovetzki R, Levitan I. Use of cyclodextrins to manipulate plasma membrane cholesterol content: evidence, misconceptions and control strategies. Biochim Biophys Acta. 2007; 1768(6):1311–1324. [PubMed: 17493580]
25. Davis SJ, van der Merwe PA. The kinetic-segregation model: TCR triggering and beyond. Nat Immunol. 2006; 7(8):803–809. [PubMed: 16855606]
26. McKeithan TW. Kinetic proofreading in T-cell receptor signal transduction. Proc Natl Acad Sci U S A. 1995; 92(11):5042–5046. [PubMed: 7761445]
27. Valitutti S, Muller S, Cella M, Padovan E, Lanzavecchia A. Serial triggering of many T-cell receptors by a few peptide-MHC complexes. Nature. 1995; 375(6527):148–151. [PubMed: 7753171]
28. Daniels MA, et al. Thymic selection threshold defined by compartmentalization of Ras/MAPK signalling. Nature. 2006; 444(7120):724–729. [PubMed: 17086201]
29. Davis MM, et al. T cells as a self-referential, sensory organ. Annu Rev Immunol. 2007; 25:681–695. [PubMed: 17291190]
30. Henrickson SE, et al. T cell sensing of antigen dose governs interactive behavior with dendritic cells and sets a threshold for T cell activation. Nat Immunol. 2008; 9(3):282–291. [PubMed: 18204450]

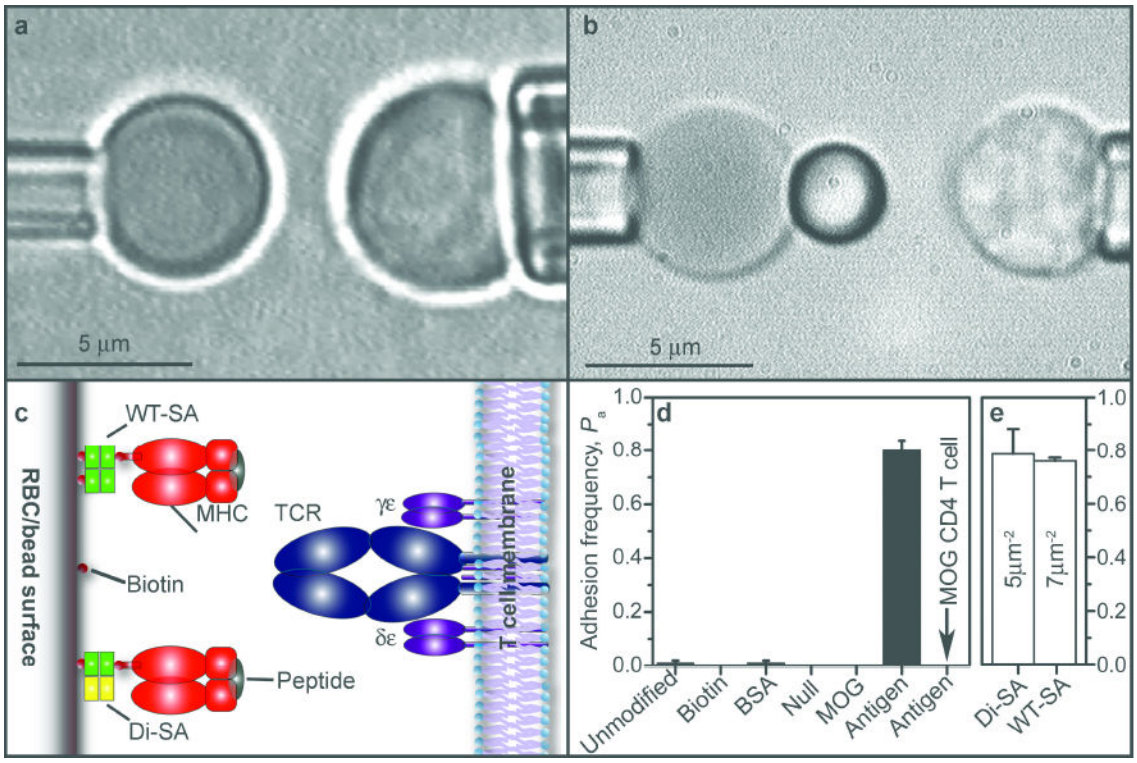

Figure 1.

Micropipette and BFP. **a** and **b**, Micrographs of the micropipette (**a**) and BFP (**b**). A T cell (*right*) aspirated by a pipette was aligned with a RBC held stationary by another pipette (*left*) without (**a**, Movie M1) or with (**b**, Movies M2 and M3) a bead attached to the apex. **c**, RBCs or beads (*left*) were coupled by WT-SA or Di-SA[10] with monomeric pMHC to interact with the TCR on T cells (*right*). **d**, Specificity controls of adhesion frequency measured at 5 s between OT1 T cells and unmodified RBCs, biotinylated RBCs without coating, biotinylated RBCs coated with BSA, null pMHC-I (VSV:H-2K^b), pMHC-II (MOG:I-A^b) or antigenic pMHC-I (OVA:H-2K^b), or between MOG CD4+ T cells and biotinylated RBCs coated with OVA:H-2K^b. **e**, Comparison between adhesion frequencies measured at 2 s using 7 and 5 μm^{-2} pMHC respectively captured by WT-SA and Di-SA.

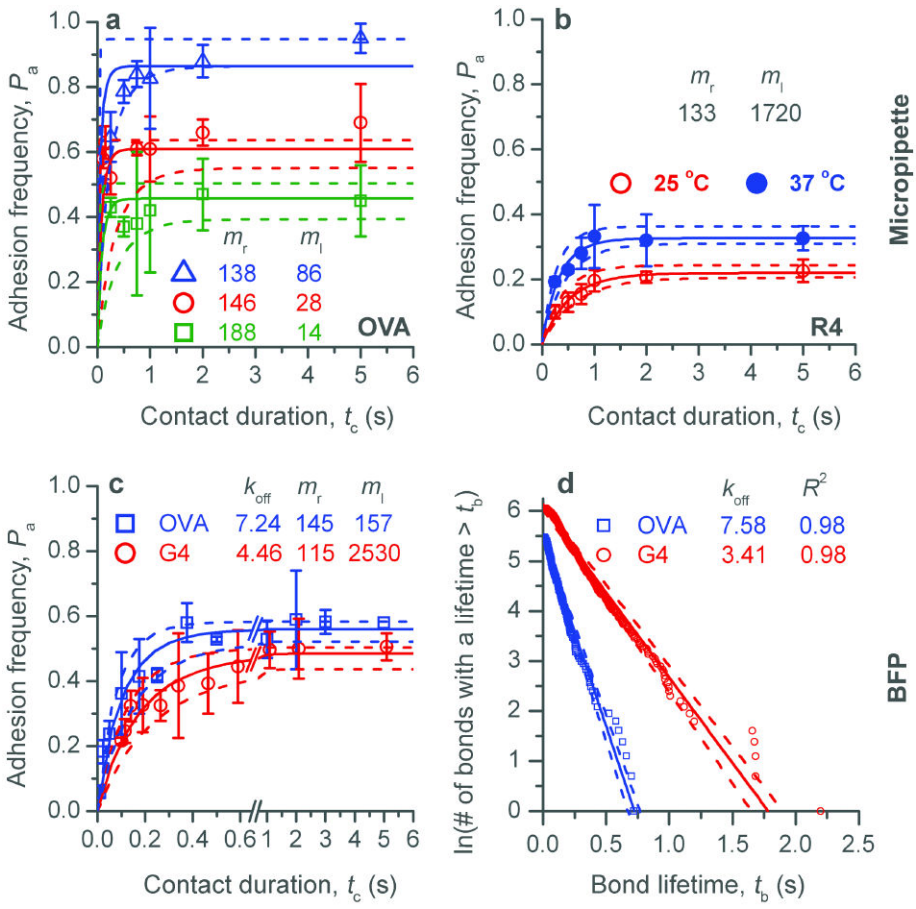

Figure 2.

2D kinetics measurements. **a** and **b**, Adhesion curves for the OT1 TCR interacting with OVA (**a**) and R4 (**b**) measured by micropipette at 25 °C (**a**) or both 25 and 37 °C (**b**) at indicated site densities. **c**, Adhesion curves of the OT1 TCR interacting with OVA and G4 measured by BFP at 25 °C. The data (points) were fitted (color matched solid curves) by a model for 2D binding kinetics[5] (**a**, **b** and **c**). **d**, Pooled ensembles of 239 (OVA) or 424 (G4) lifetimes of bonds between the OT1 TCR and OVA (□) or G4 (○) were respectively sorted according to their durations. For each peptide, the natural log of the number of events with a lifetime ≥ t_b was plotted vs. t_b and fitted by a straight line. The negative slope represents off-rate k_{off} (indicated). The goodness-of-fit was indicated by the R^2 values. Color matched dotted curves represent 95% confidence intervals of the best-fit curves obtaining by bootstrapping.

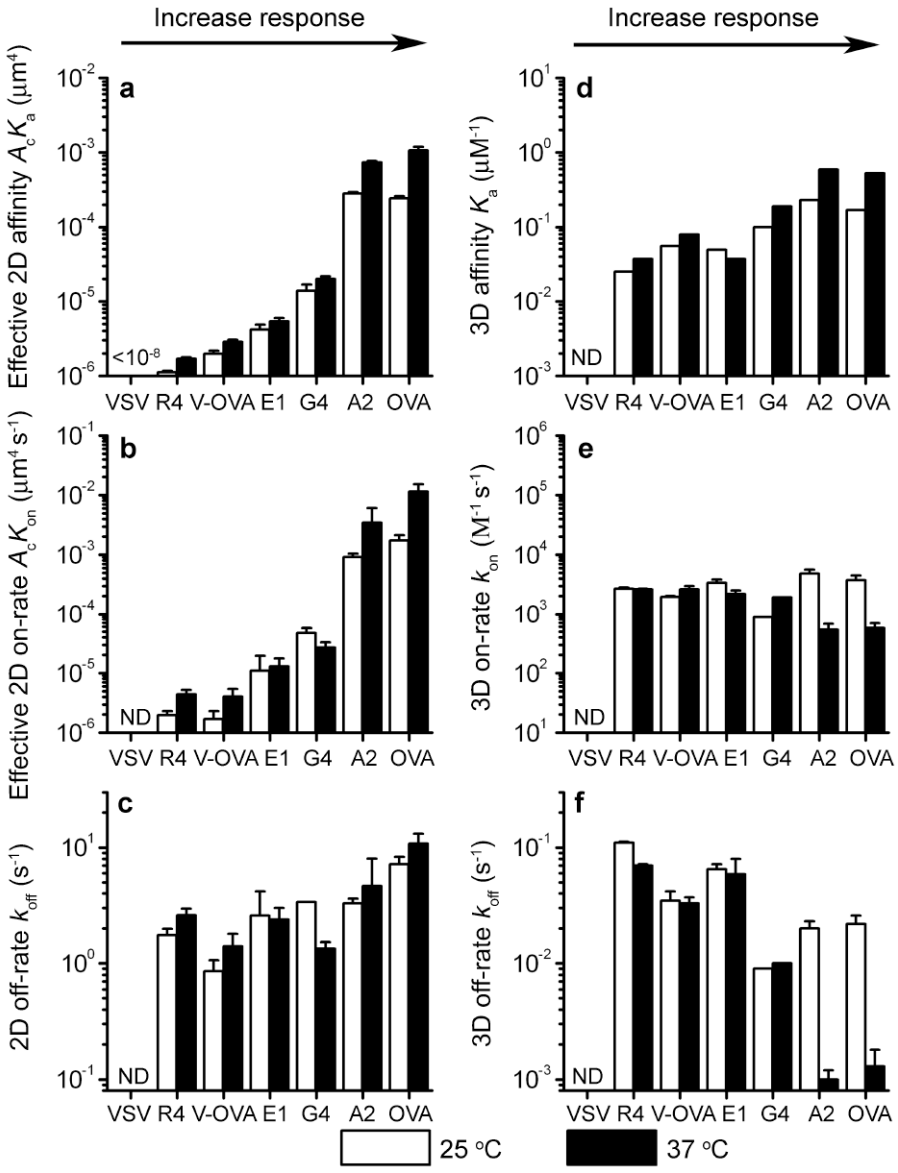

Figure 3.

Comparison of 2D and 3D kinetics. Affinities (**a** and **d**), on-rates (**b** and **e**), and off-rates (**c** and **f**) of the OT1 TCR interacting with indicated pMHCs. The 2D data (**a-c**) were measured by the adhesion frequency assay and analyzed with a monomeric binding model. The 3D data (**d-f**) from Refs. 11,12 were measured by surface plasmon resonance and analyzed with the same monomeric binding model except for the OVA and A2 data at 37 °C, which were analyzed with a dimeric binding model (values of the second-step kinetics were plotted).

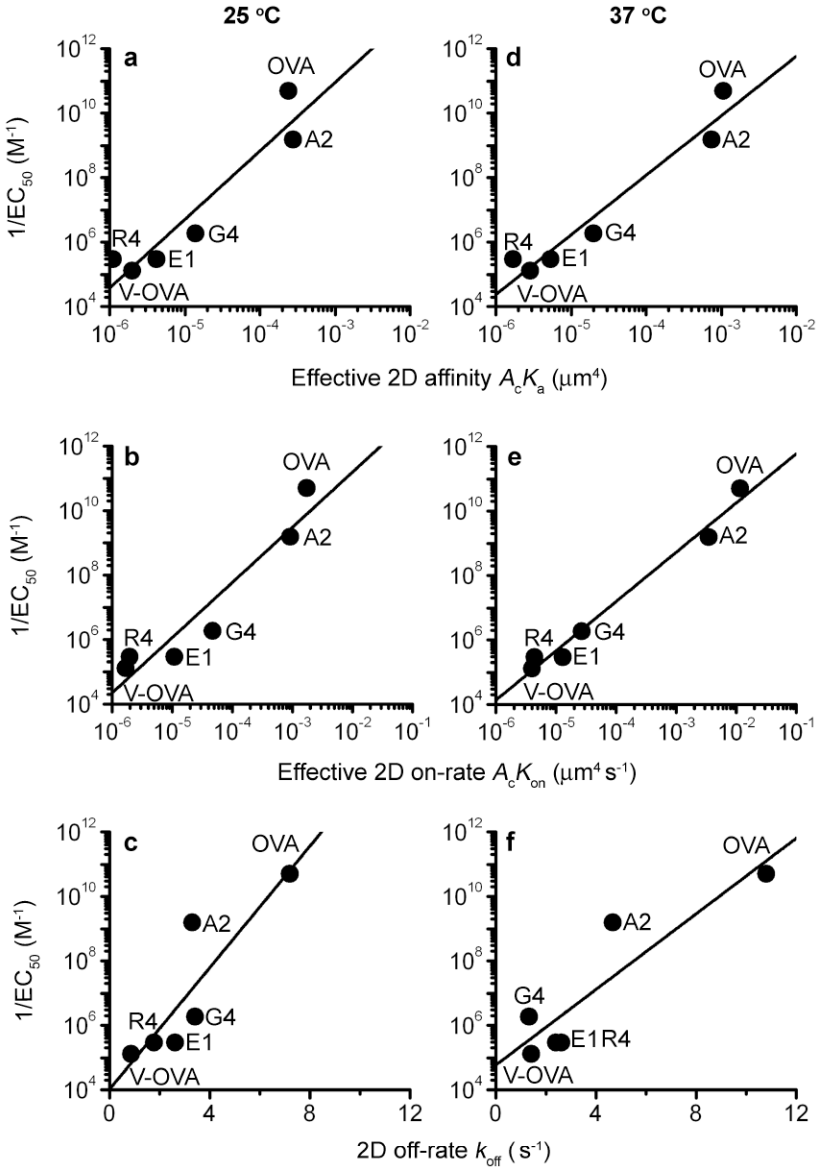

Figure 4.

Correlation between 2D kinetics and T cell proliferation. The reciprocal concentration required to reach half-maximal T cell proliferation ($1/EC_{50}$) is plotted vs the effective 2D affinity (**a** and **d**), on-rate (**b** and **e**), and off-rate (**c** and **f**) measured at 25 °C (**a-c**) or 37 °C (**d-f**) for the indicated peptides. To quantify T cell proliferation, naïve OT1 splenocytes (3×10^5/well) were cultured in 96-well plates with the indicated peptides at 37°C. After 48 h, 0.4 μCi/well of [^{3}H] thymidine was added. After another 18 h, cells were harvested on a FilterMate harvester (PerkinElmer) and analyzed on a Matrix 96 Direct Beta Counter (PerkinElmer). EC_{50} values were calculated using GraphPad Prism.

Table 1

Summary of 2D Kinetic Rates and Binding Affinities of OTI TCR-pMHC Interactions

Peptide	Sequence	Mature T cell Activation	A_cK_{on}(μm^{4}s^{-1})		K_{off}(s^{-1})		A_cK_a (μm^4)	
			25 °C	37 °C	25 °C	37 °C	25 °C	37 °C
OVA	SIINFEKL	Antigen	1.7 ± 0.4 (×10^{-3})	1.2 ± 0.4 (×10^{-2})	7.2 ± 1.1	10.8 ± 2.3	2.4 ± 0.2 (×10^{-4})	1.1 ± 0.1 (×10^{-3})
A2	SAINFEKL	Agonist	9.2 ± 1.2 (×10^{-4})	3.5 ± 2.6 (×10^{-3})	3.3 ± 0.3	4.7 ± 3.4	2.8 ± 0.1 (×10^{-4})	7.4 ± 0.3 (×10^{-4})
G4	SIIGFEKL	Weak ag./antag.	4.7 ± 1.0 (×10^{-5})	2.7 ± 0.6 (×10^{-5})	3.4 ± 0.0	1.3 ± 0.2	1.4 ± 0.3 (×10^{-5})	2.0 ± 0.2 (×10^{-5})
E1	EIINFEKL	Weak ag./antag.	1.1 ± 0.9 (×10^{-5})	1.3 ± 0.5 (×10^{-5})	2.6 ± 1.6	2.4 ± 0.6	4.2 ± 0.7 (×10^{-6})	5.4 ± 0.6 (×10^{-6})
V-OVA	RGYNYEKY	Antagonist	1.7 ± 0.6 (×10^{-6})	4.0 ± 1.4 (×10^{-6})	0.9 ± 0.2	1.4 ± 0.4	2.0 ± 0.2 (×10^{-6})	2.9 ± 0.2 (×10^{-6})
R4	SIIRFEKL	Antagonist	2.0 ± 0.3 (×10^{-6})	4.4 ± 0.8 (×10^{-6})	1.8 ± 0.2	2.6 ± 0.4	1.1 ± 0.1 (×10^{-6})	1.7 ± 0.1 (×10^{-6})
VSV	RGYVYQGL	Null	ND	ND	ND	ND	<10^{-8}	<10^{-8}

ND = Not Detectable